Japanese Journal of Radiology (2019) 37:555–563
https://doi.org/10.1007/s11604-019-00843-1

ORIGINAL ARTICLE

Safety margin of radiofrequency ablation for hepatocellular carcinoma: a prospective study using magnetic resonance imaging with superparamagnetic iron oxide

Kuniaki Fukuda[1] · Kensaku Mori[2] · Naoyuki Hasegawa[1] · Katsuhiro Nasu[2] · Kazunori Ishige[1] · Yoshikazu Okamoto[2] · Masanari Shiigai[3] · Masato Abei[1] · Manabu Minami[2] · Ichinosuke Hyodo[1]

Received: 21 December 2018 / Accepted: 8 May 2019 / Published online: 17 May 2019

Abstract

Purpose In radiofrequency ablation (RFA) for hepatocellular carcinoma (HCC), it is difficult to assess the ablative margin (AM) precisely by comparing pre- and post-RFA CT images. We prospectively studied the AMs using magnetic resonance imaging (MRI) with pre-administered superparamagnetic iron oxide (SPIO). SPIO is safe for kidney disease patients.

Materials and methods Hepatocellular carcinoma patients were treated with RFA within 8 h of SPIO administration. On T2*-weighted MRI performed 4–7 days later, AM was visualized as a hypointense rim. The ablation status was classified as AM(+) if the rim completely surrounded the tumor, AM(0) if the rim was partly discontinuous without tumor protrusion, and AM(−) if the rim was partly discontinuous with tumor protrusion. The minimal thickness of AM was measured. AM(−) tumors were re-treated consecutively.

Results In total, 85 HCCs ablated in 76 patients were evaluated. The local recurrence rate at 3 years was 2% for AM(+) tumors and 34% for AM(0) tumors ($p < 0.01$). In addition, no local recurrence was seen in the tumors with an AM of ≥ 2 mm.

Conclusion MRI with pre-administered SPIO is useful for determining the AM precisely, and an AM of ≥ 2 mm is recommended for curative RFA.

Trial registration number This study was registered with UMIN Clinical Trials Registry (UMIN 000025406).

Keywords Hepatocellular carcinoma · Radiofrequency ablation · Superparamagnetic iron oxide · Ablative margin

Introduction

Radiofrequency ablation (RFA) is widely used as a standard therapy for early-stage hepatocellular carcinoma (HCC). Although RFA is less invasive than hepatic resection, [1, 2] local recurrence has been reported more frequently after RFA than after hepatic resection in several randomized control trials [3, 4]. To avoid local recurrence, a minimum ablative margin (AM) of 5 mm thickness, as estimated on contrast-enhanced computed tomography (CECT), has been recommended in several studies [1, 5]. However, it is theoretically difficult to measure the AM thickness objectively using CECT. In the first place, we cannot distinguish the AM from the ablated tumor, because both appear as a single low-density areas lacking contrast enhancement. The technique currently accepted for the assessment of the AM involves comparing the CECT images acquired before and after RFA by visual inspection, and estimating the invisible AM thickness subjectively. This theoretical flaw of CECT results in over or underestimation of the AM. Overestimation of the AM can lead to inadequate treatment, resulting in a higher local recurrence rate. In contrast, underestimation can lead to unnecessary additional treatment in patients with chronic liver disease. Thus, there is an urgent need for a new imaging method to measure the AM precisely.

Kuniaki Fukuda and Kensaku Mori contributed equally.

✉ Kuniaki Fukuda
k-fukuda@md.tsukuba.ac.jp

[1] Department of Gastroenterology, Institute of Clinical Medicine, Faculty of Medicine, University of Tsukuba, Tennodai 1-1-1, Tsukuba, Ibaraki 305-8575, Japan

[2] Department of Radiology, Faculty of Medicine, University of Tsukuba, Ibaraki, Japan

[3] Department of Radiology, Tsukuba Medical Center Hospital, Ibaraki, Japan

An evaluation method using magnetic resonance imaging (MRI) with pre-administered superparamagnetic iron oxide (SPIO) can clearly distinguish the AM from both the surrounding liver parenchyma and the ablated tumor [6]. SPIO is a contrast medium that is taken up by Kupffer cells and attenuates the MR signal with respect to the liver parenchyma. Malignant hepatic tumors do not contain Kupffer cells, thus show hyperintensity. The signals of liver parenchyma significantly decrease for 8 h and 2 days after the administration of SPIO at doses 5 and 10 μmol/kg, respectively [7]. Thus, at a clinical dose of 8 μmol/kg, the signal decay lasts significant at least for 8 h but becomes insignificant 2 days later. When RFA is performed within 8 h after SPIO injection, only the liver parenchyma surrounding a tumor, namely the AM, show hypointense rim after 2 or more days on T2*-weighted images on non-enhanced MRI, because the Kupffer cells in the AM are damaged and unable to excrete SPIO. The strength of our method is that it enables precise measurement of the AM without the need for comparison with other images.

In the present study, we prospectively investigated the usefulness of MRI with pre-administered SPIO for determination of the AM, and compared it with that of contrast-enhanced CT. We also determined the minimum AM thickness that may be deemed suitable for curative HCC ablation.

Materials and methods

Patients

This prospective study was approved by the institutional ethics committee (H19-208) and was conducted in accordance with the ethical standards of the Declaration of Helsinki. HCC patients with a planned RFA were invited to participate in this study if they satisfied a predetermined set of criteria. All patients who agreed to be involved in the study were enrolled after obtaining written informed consent from them. The inclusion criteria were as follows: (a) age ≥ 20 years (b) ability to follow instructions during treatment (c) Child–Pugh grade A or B (d) no significant ascites (e) tolerance to CECT (f) tolerance to SPIO-enhanced MRI (g) 3 or fewer hypervascular HCCs measuring 3 cm or less in diameter (h) HCCs with no vascular invasion (i) previously untreated nodule/s and (j) HCCs detectable by ultrasonography (US). A hypervascular HCC was diagnosed using CECT when a nodule was enhanced during the arterial phase and showed washed-out patterns during the venous/late phase. The exclusion criterion was HCCs that showed signal decay on SPIO-enhanced MRI, because the AM assessment would be difficult for such tumors.

Patient background and laboratory data were recorded before RFA; these included age, sex, liver-disease etiology, levels of tumor markers (alpha-fetoprotein and des-gamma-carboxyprothrombin), tumor status, and Child–Pugh score.

MRI and CT

Patients were examined using a 1.5-T MR imaging unit (Gyroscan Intera; Philips Medical Systems, Best, Netherlands) equipped with phased-array synergy-body coils. Pre-RFA MRI using SPIO (Resovist; FUJIFILM RI Pharma, Tokyo, Japan) was performed within 8 h (approximate range 2–6 h) of RFA on the same day, because the SPIO-derived signal decay of the normal liver lasted for approximately 8 h.

After the acquisition of unenhanced axial T1, T2, and diffusion-weighted images, 8 μmol Fe/kg body weight of SPIO was administered intravenously. Ten minutes later, an axial SPIO-enhanced T2*-weighted three-dimensional sensitivity-encoding water-excitation multishot echo-planar (3D-SWEEP) sequence (repetition time/echo time/flip angle = 37 ms/13 ms/25°; matrix = 192 × 512; EPI factor = 9; binomial 1–3–3–1 pulses for water excitation) was obtained [8]. In this sequence, a total of 72 axial images of 2.5 mm thickness could be acquired within 17 s during a single breath hold, and multiplanar images could be reconstructed. For post-RFA MRI, besides axial T1- and T2-weighted images, unenhanced 3D-SWEEP sequence with the same parameters as the pre-RFA MRI were acquired 4–7 days later. This is because the signal of the non-ablated liver parenchyma returns to the normal level, due to the excretion of SPIO, in 2 days or more after administration.

Unenhanced and triphasic CECT of the upper abdomen were performed before RFA and within 2 weeks of RFA, using a 64- or 256-detector row CT scanner (Brilliance 64 CT scanner or Brilliance iCT; Philips Medical Systems, Best, Netherlands). The contrast material was injected into the antecubital vein at a rate of 4 mL/s. Arterial-phase images were acquired 15 s after the attenuation of a region of interest located in the abdominal aorta exceeded 150 Hounsfield Units during bolus tracking. Portal and delayed phase images were acquired at 50 s and 160 s after the beginning of arterial phase image acquisition. All CT images were reconstructed consecutively at 2-mm thickness.

RFA

RFA was performed using the Cool-Tip RF ablation system (Covidien; Medtronic, Fridley, MN, USA) under US guidance (Logiq 9; GE Healthcare Japan, Tokyo, Japan). A volume navigation system (VNAV; GE Healthcare Japan) was used to guide the ablation of the HCC, which was difficult to detect clearly by US alone. After insertion of the electrode needle (17-gauge with a 2–3 cm exposed metallic tip) into the tumor, a radiofrequency current was applied, and its power was increased until the impedance rose to

10–20 Ω above the baseline level. To avoid a further increase in tissue temperature, which would probably have resulted in charring, the power was reduced automatically to 10 W, and this series of treatments were performed once or twice for each tumor. The tumors were treated using a single insertion of the electrode needle, and additional insertions were performed only when treatment by a single insertion was deemed insufficient. Three hepatologists performed RFA for all the patients.

Image analysis

One of five board-certified radiologists who specialize in body imaging were randomly assigned to evaluate the MR images after RFA. Using three-dimensional data and multiplanar reconstruction images, the ablation status was classified into 1 of the following 3 types: AM(+) when the hypointense rim completely surrounded the tumor; AM(0) when the hypointense rim was partly discontinuous, without the protrusion of the tumor beyond the postulated border of the ablated area; AM(–) when the hypointense rim was partly discontinuous, with protrusion of the tumor. An AM that was discontinued by a vessel adjacent to the tumor was classified as AM(0). In cases of AM(+), the minimum thickness of the AM was measured by the radiologist to determine the optimal AM thickness (Fig. 1). CECT scans obtained after RFA were also prospectively evaluated by one of the board-certified radiologists at our institution who did not evaluate the MR images of the same patient. The ablation status was then classified as 1 of the following 3 types: good (the tumor enhancement disappeared on the post-RFA CT images, and the non-enhanced ablated area seemed to cover the area of tumor enhancement with a safety margin of 1 mm or more on the pre-RFA CT images); fair (the tumor enhancement disappeared, but the non-enhanced area seemed to cover the tumor marginally with a safety margin of less than 1 mm on the pre-RFA CT images); poor (the tumor enhancement persisted on the post-RFA CT images). The post-RFA CT images were compared with the pre-RFA CT images using visual registration. Specialized software was not used to overlay the images.

Follow-up protocol

After RFA, all patients were examined using CECT or MRI every 3 months for the first year. After this, imaging studies including US, were performed every 2–4 months. Patients with treated HCCs classified as AM(0) underwent additional imaging studies within a month of RFA, because the risk of local recurrence was considered to be high. Patients with AM(−) HCCs received additional treatments during the same hospitalization period. Local recurrence was defined as a new hypervascular lesion detected in the ablated area or in its boundary. To evaluate the influence of MRI with pre-administered SPIO on liver function, the Child–Pugh scores recorded before RFA were compared with those recorded 6 months after RFA.

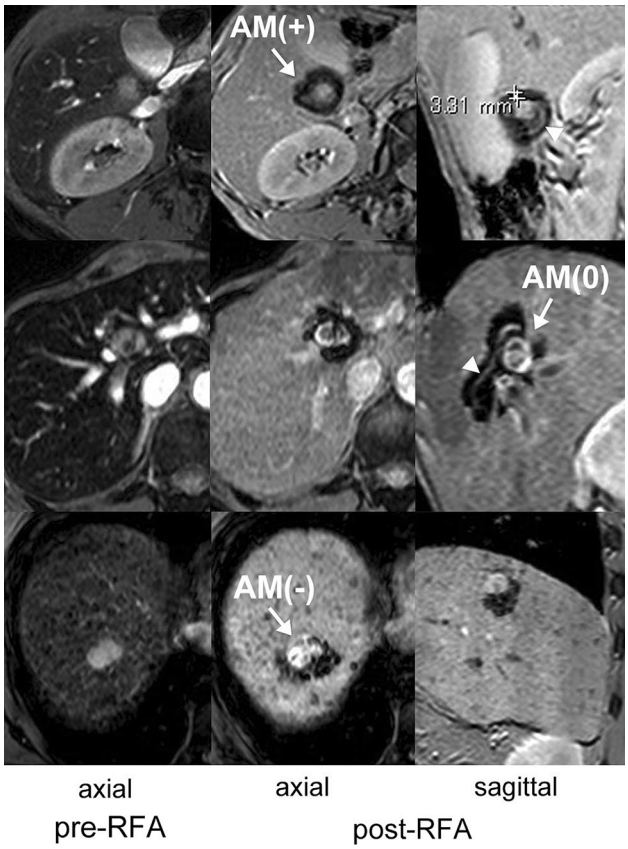

Fig. 1 Images corresponding to each ablation status determined on the basis of MRI with pre-administered SPIO before and after RFA for small nodular HCCs. Axial views of pre-RFA SPIO-MRI (left), axial views of post-RFA non-contrast MRI (center), and sagittal views of post-RFA non-contrast MRI (right) are shown. The quality of ablation was categorized as AM(+) (upper row), AM(0) (middle row), or AM(−) (lower row). Arrows of AM(0) and AM(−) show the regions lacking the AM. Curvilinear hyperintense artifacts are indicated by arrowheads on the right-hand images in the upper and middle rows. *MRI* magnetic resonance imaging, *SPIO* superparamagnetic iron oxide, *RFA* radiofrequency ablation, *HCC* hepatocellular carcinoma, *AM* ablative margin

Statistical analysis

The intervals from RFA to post CECT and unenhanced MRI were compared using a paired *t* test. Intermodality agreement for AM assessment between MRI and CT was assessed using κ statistics: moderate ($\kappa = 0.41$–0.60); good ($\kappa = 0.61$–0.8); or excellent ($\kappa = 0.81$–1.0). Local recurrence rates were calculated using the Kaplan–Meier method. The difference in local recurrence according to each condition was evaluated using the log-rank test. A *p* value of less than

0.05 was considered statistically significant. All statistical analyses were performed using the SPSS 21.0 statistical software (IBM, New York).

Results

Clinical characteristics of patients and tumors

From April 2008 to December 2015, 78 consecutive patients with 88 hypervascular HCCs met the inclusion criteria. Three HCCs in 2 patients were excluded because the HCC nodules also showed signal decay on SPIO-enhanced MRI, and the AM could not be evaluated. Thus, the final study population comprised 76 patients, with 85 hypervascular HCCs. The patient and tumor characteristics are summarized in Table 1.

Safety of RFA for the SPIO-enhanced liver

All 76 patients tolerated pre-RFA CECT and SPIO-enhanced MRI, RFA in the SPIO-enhanced liver and post-RFA CECT and unenhanced MRI. The interval from RFA to post-RFA CECT and unenhanced MRI ranged from 4 to 7 days (mean ± SD of 5.2 ± 1.2 days) and from 4 to 11 days (mean ± SD 5.3 ± 0.7 days), respectively. There was no significant difference between these intervals ($p = 0.315$). The diameter of the target HCCs ranged from 8 to 30 mm (median of 15 mm). The number of RFA needle insertions were 1 for 80 tumors and 2 for 5 tumors (mean ± SD of 1.06 ± 0.26). No serious adverse events occurred after RFA in the SPIO-enhanced liver. One patient had a late adverse event of local bile duct stenosis near the ablation site, but his liver function did not decrease in the absence of treatment. Six months after RFA, the Child–Pugh score increased by 1 in 10 patients (13%), remained unchanged in 48 patients (63%), decreased by 1 in 16 patients (21%) and decreased by 2 in 2 patients (3%). The change in the Child–Pugh score was − 0.13 ± 0.66 (mean ± SD).

Table 1 Clinical characteristics of patients and tumors

	Total (76 patients, 85 tumors)
Age (years)	
Median (range)	71 (53–88)
Gender, *n* (%)	
Male/female	53 (70.0)/23 (30.0)
Etiology, *n* (%)	
HCV/HBV/other	60 (79.0)/8 (10.5)/8 (10.5)
Prior treatment, *n* (%)	
No/yes	25 (32.9)/51 (67.1)
Serum AFP (ng/mL), *n* (%)	
Median (range)	9 (1–527)
Serum DCP (mAU/mL), *n* (%)	
Median (range)	28 (8–11,245)
Child–Pugh grade, *n* (%)	
A/B	54 (71.1)/22 (28.9)
Tumor number, *n* (%)	
1/2	67 (88.2)/9 (11.8)
Tumor size (mm), *n* (%)	
Median (range)	15 (8–30)

HCV hepatitis C virus, *HBV* hepatitis B virus, *AFP* alpha-fetoprotein, *DCP* des-gamma-carboxyprothrombin

Ablation status

The ablation status evaluated on MRI was AM(+) for 50 HCC nodules (59%), AM(0) for 24 (28%), and AM(−) for 11 (13%). Of the 50 AM(+) tumors, 47 were ablated using a single needle insertion and the other 3 needed 2 needle insertions. In the AM(+) tumors, the average minimal AM thickness was 2.6 ± 1.5 mm, and 6 of the 50 tumors (12%) were ablated with a minimal AM thickness of ≥ 5 mm (Fig. 2). Of the 11 AM(−) tumors, 10 were re-treated using RFA. The remaining HCC that could not be ablated with this re-treatment was subsequently treated using transarterial-chemoembolization (TACE). The ablation status on CT was "good" for 58 HCC nodules (68%), "fair" for 18 (21%), and

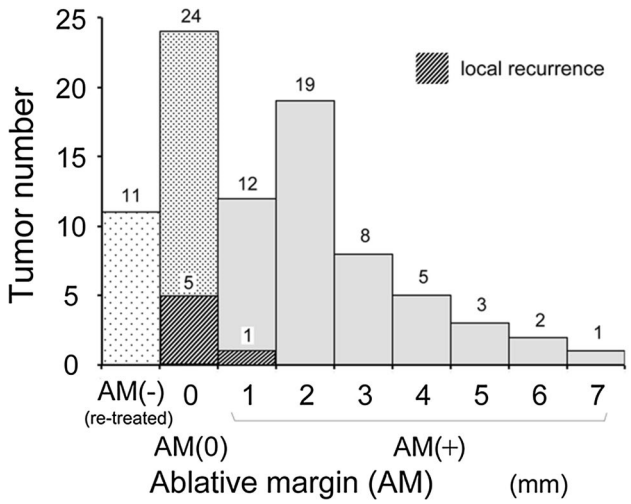

Fig. 2 Distribution of the minimal ablative margin detected by MRI with pre-administered SPIO after RFA for HCC. The minimal AM determined using MRI with pre-administered SPIO after RFA for HCC was measured for all tumors. An AM of 0 mm was classified as AM(0), and a negative AM was classified as AM(−).The parts of the graph marked with oblique lines show the number of local recurrences. Note that the HCCs classified as AM(−) were re-treated immediately, thus no local recurrence was observed. *MRI* magnetic resonance imaging, *SPIO* superparamagnetic iron oxide, *RFA* radiofrequency ablation, *HCC* hepatocellular carcinoma, *AM* ablative margin

Table 2 Comparison of the status of the ablative margin between SPIO-MRI and CT after RFA for HCC

	CT			Total
	Good	Fair	Poor	
SPIO-MRI				
AM(+)	42 [1]	5	3	50
AM(0)	13 [3]	11 [2]	0	24
AM(–)	3	2	6	11
Total	58	18	9	85

[ ] Number of local recurrences

SPIO superparamagnetic iron oxide, *MRI* magnetic resonance imaging, *CT* computed tomography, *RFA* radiofrequency ablation, *HCC* hepatocellular carcinoma, *AM* ablative margin

"poor" for 9 (11%). Table 2 presents a comparison of MRI and CT evaluation of the ablation status. The intermodality agreement rate was 69% (59/85), and the κ coefficient was 0.418, indicating moderate agreement. With the MRI as the reference standard, the ablation status was overestimated by CT in 21% of the tumors (18/85) and underestimated by CT in 9% (8/85). Actual MR and CT images judged to indicate different ablation statuses are shown in Fig. 3 and 4. The tumor shown in Fig. 3 was judged as having a "good" ablation status on CECT but classified as AM(0) on MRI. Local recurrence occurred in this case 14 months after RFA. In another case, the tumor was judged as having a "poor" ablation status on CECT but classified as AM(+) on MRI (Fig. 4). Local recurrence had not occurred more than 3 years after RFA, in this case.

Local recurrence rates and the cutoff value for the AM thickness

Of the 85 ablated HCCs, 6 tumors recurred locally in the median observation period of 40 months (95% confidence interval [CI], 27.2–52.9 months). Five of these were classified as AM(0) and 1 was classified as AM(+) with a minimum AM of 1 mm (Fig. 2). On CECT, 2 tumors were classified as 'fair' and 4 were classified as 'good'. The 3-year local recurrence rates of AM(+) and AM(0) tumors were 2% (95% CI 0–4%) and 34% (95% CI 21–47%), respectively (log-rank test, $p < 0.01$) (Fig. 5). No local recurrence was observed in the AM(−) HCCs, which were immediately re-ablated in the first RFA session ensuring an adequate AM.

Discussion

The results of the present study showed that successful tumor ablation using RFA is ensured when the AM is a minimum of 2 mm on MRI with pre-administered SPIO. To date,

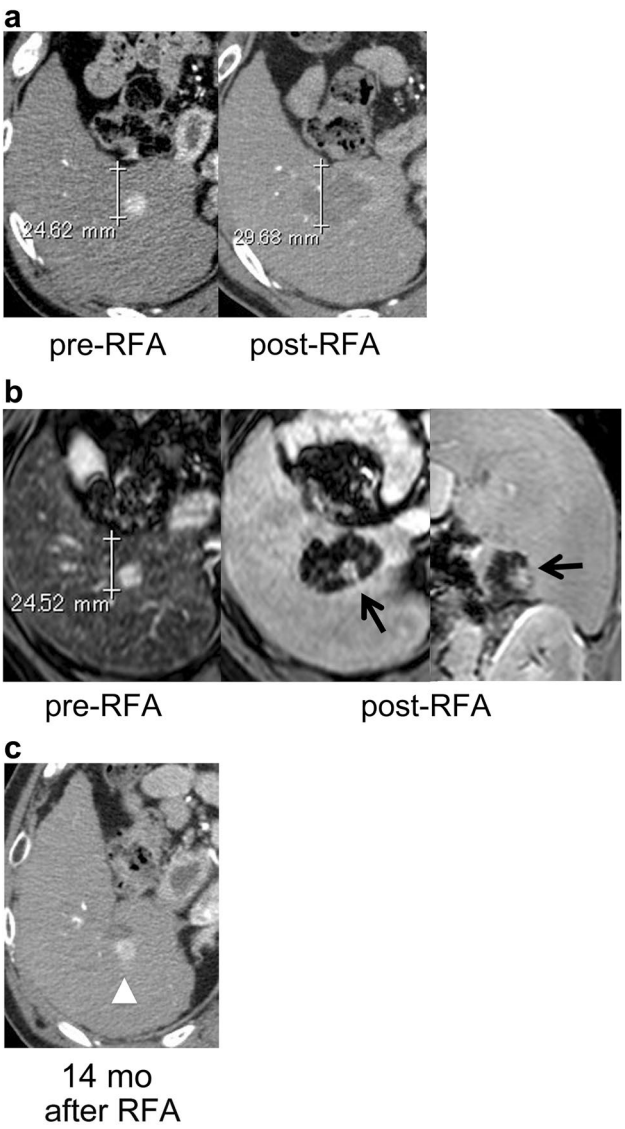

Fig. 3 A case in which the ablation status was judged as good on CT but AM(0) on MRI. **a** The early enhancement of the tumor completely disappeared on the post-RFA CT images, and the tumor seemed to be treated with an adequate AM. The ablation status was judged as "good". **b** The tumor just reached the posterior boundary of the ablated area (arrows) in the post-RFA MR image, and the ablation status was judged as AM(0). The right-hand post-RFA image shows the sagittal view. **c** HCC recurrence was observed at the point of the ablated area indicated with an arrowhead at 14 months after RFA. *CT* computed tomography, *AM* ablative margin, *MRI* magnetic resonance imaging

a rather thick AM has been recommended when administering RFA for HCCs, based on a report that micro-satellite lesions can exist near the tumor [9]. When HCCs are treated using radical hepatic resection, the resected margin can be measured accurately using pathological examination, and some reports have shown that the thickness of the surgical margin does not affect HCC recurrence or patient survival [10, 11]. The minimum AM applied in hepatic resection may

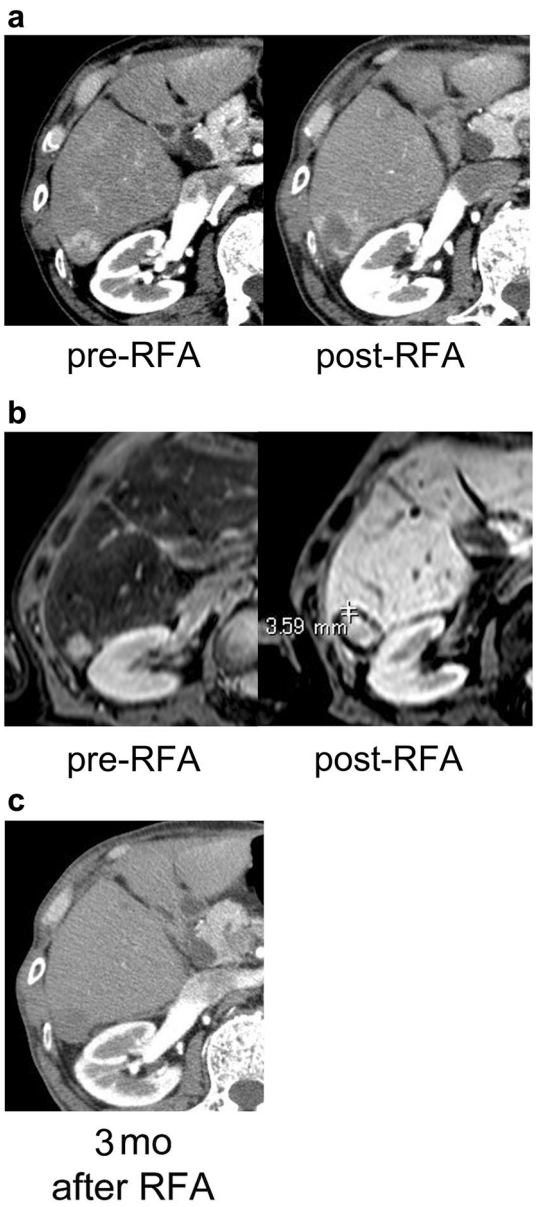

Fig. 4 A case in which the ablation status was judged as poor on CT but AM(+) on MRI. **a** The early tumor enhancement of HCC seemed to persist on the post-RFA CT image, and the ablation status was judged as 'poor'. **b** The black rim of the AM completely encircled the tumor on the post-RFA MR image, and the status was judged as AM(+). **c** An arterial phase CT image 3 month after RFA. No local recurrence was observed 3 years after RFA without additional treatments. *CT* computed tomography, *AM* ablative margin, *MRI* magnetic resonance imaging, *HCC* hepatocellular carcinoma, *RFA* radiofrequency ablation

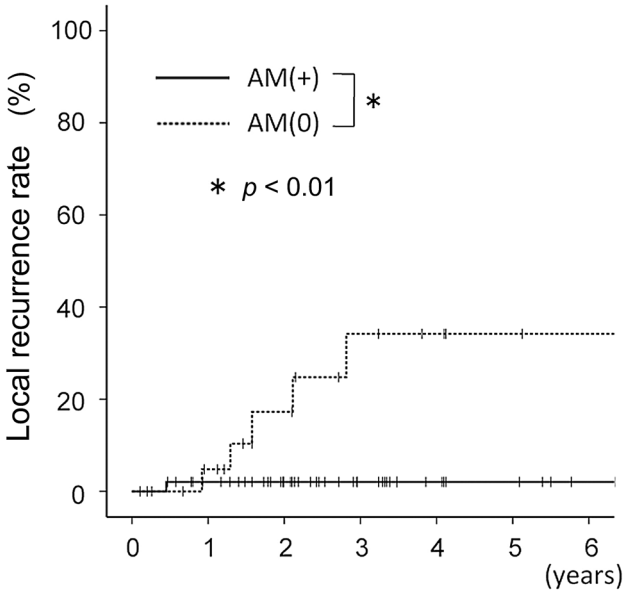

Fig. 5 Kaplan–Meier estimates of local recurrence for HCCs treated by RFA. Local recurrence rates according to the categories AM(+) (solid line) and AM(0) (broken line) classified by MRI with pre-administered SPIO. *HCC* hepatocellular carcinoma, *RFA* radiofrequency ablation, *AM* ablative margin, *MRI* magnetic resonance imaging, *SPIO* superparamagnetic iron oxide

be acceptable, provided it is accurately assessed using MRI with pre-administered SPIO. In the present study, an intermodality disagreement between MRI and CT with respect to the ablation status was observed in several patients after RFA. This discrepancy might be related to the limitations of comparative review of CECT images recorded before and after RFA. As mentioned in the introduction, the theoretical flaw of CECT is that the ablated HCC disappears in the ablated area after RFA, resulting in the subjective estimation of the AM. The image overlay technique would be useful to visualize the AM; nevertheless, even minimal misregistration could lead to misjudgment of the AM state. Furthermore, periablational enhancement, which may be judged as the remaining early enhancement of the HCC, sometimes appears after RFA, as shown in Fig. 4. Our method has two advantages addressing these two drawbacks of CECT assessment. First, our method can distinguish the AM from the ablated tumor on a single image, without comparing two different images nor using any image overlay technique. Second, our method detects the remaining SPIO in the AM, and thus is not affected by hepatic blood flow.

Preservation of liver function is important to prolong the survival of patients receiving HCC treatment [12]. Some investigators have recommended that a safe AM is 5 mm or more to prevent local recurrence after RFA [1, 5]. A local recurrence rate of cases classified as 'good' on CECT is high in this study because the ablation status was defined as 'good' when a safety margin seemed 1 mm or more. This means, however, that a few rounds of needle insertions for RFA are often necessary to obtain an adequate AM on CT. Wider ablation increases the risk of complications and liver damage. Precise three-dimensional AM assessment using MRI with pre-administered SPIO

allows the size of the ablation area to be optimized, resulting in minimization of both local recurrence and damage to the normal liver parenchyma. In fact, our study demonstrated a sufficiently low local recurrence rate in AM(+) tumors without a substantial increase in the Child–Pugh score (-0.13 ± 0.66), and more than half of the total number of tumors (47/85) could be ablated achieving AM(+) status with just a single needle insertion.

Recently, the clinical usefulness of our evaluation method has been demonstrated in a study by another group [13]. However, over one-third of the patients in that study were treated with RFA combining TACE, thus strictly speaking, the results were not valid for investigating the relationship between the AM and the local recurrence rate after RFA alone. In addition, they did not measure the AM thickness. Our study is the first report to investigate the relationship between the objectively measured AM thickness and the local recurrence rate after RFA alone.

To assess the exact AM after RFA, various new methods have recently been proposed. As mentioned before [13], by performing TACE before RFA, the AM can be visualized as a hypodense rim surrounding the hyperdense HCC, with iodized oil deposition on post-RFA CECT. However, for small HCCs measuring 3 cm or less, the combination therapy with TACE plus RFA and RFA alone, were reported to have similar effects on local tumor control and patient survival [14]. Thus, the combination therapy seems overzealous for small HCCs. The use of fusion images of pre- and post-RFA CT or MRI is relatively easy and objective [15–17], but misregistration artifacts are inevitable where 2 images are recorded at different times, as discussed above.

Contrast-enhanced US is a useful and safe modality. However, the time window for assessment is short, and image quality is affected by tumor location and the patient's somatotype [18]. Instead of SPIO, gadolinium-ethoxybenzyl-diethylenetriamine pentaacetic acid (Gd-EOB-DTPA) has been reported to be a useful agent that can be administered before MRI for evaluating AM after RFA, for HCCs [19]. However, because of its rapid excretion from the liver parenchyma, RFA must be performed within 1 h of administration. Moreover, the post-RFA MRI must be performed within 7 h of RFA, because the signal of ablated tumor increases due to the ablation itself on T1-weighted images, and therefore becomes difficult to distinguish from the AM thereafter. Further, there are concerns about the safety of RFA in the Gd-EOB-DTPA-enhanced liver because it remains unknown whether Gd-EOB-DTPA is chemically stable in the presence of the electrical field and high temperature. In contrast, the safety of RFA in the SPIO-enhanced liver has been experimentally established previously [20, 21]. Additionally, the conformity between the low-intensity area on MRI with pre-administered SPIO and the ablated liver parenchyma on histopathological examination has been verified in several animal studies [22, 23].

Our evaluation method has other benefits as well. First, unlike extracellular contrast agents containing iodine or gadolinium, SPIO is rarely associated with a risk of renal dysfunction and can be administered to patients with chronic renal disease [24]. Frequent CECT examinations carry the risk of renal damage and radiation exposure. In addition, acute kidney injury occurs in approximately 20% of hospitalized patients with cirrhosis, and renal dysfunction is a powerful predictor of death in cases of decompensated cirrhosis [25, 26]. Preventing renal failure is an important consideration in prolonging the survival of HCC patients with cirrhosis. Second, MRI with pre-administered SPIO accurately shows the positional relationship between the target tumor and the ablated area in a single MR study without the need to compare the findings with those of previous imaging studies. Consequently, repeated RFA as an additional therapy can be easily performed when the status is assessed to be AM(−). The detection of recurrent HCC after RFA is a challenge in diagnostic imaging. On CE-CT, the recurrent HCC is difficult to be differentiated from reactive hyperemia after RFA, because it was reported to show typical enhancement pattern (arterial enhancement with washout in portal venous phase) in only 17.5% of patients [27]. Contrast-enhanced US was reported to be impossible to identify the safety margin in 34.8% of HCC nodules after RFA, because the tumor boundary became unclear [28]. In such cases, the detection of residual HCC after RFA would be difficult. Hepatobiliary-phase images on EOB-enhanced MRI were reported not to improve but rather to degrade the accuracy for detecting recurrent HCC after RFA, because of the pseudolesions caused by a vascular abnormality [29]. Third, the obtained images can be clearly understood not only by radiologists but also physicians and even patients.

Nonetheless, this method has the following drawbacks. The sensitivity of SPIO-enhanced MRI is generally lower than that of Gd-EOB-DTPA-enhanced MRI, especially for early HCCs without early enhancement, which are often detected in the hepatobiliary phase. However, a study has reported that the survival benefit of treatment of early HCCs, without early enhancement, is marginal because of the long lead times [30]. In addition, it has been reported that the sensitivity of SPIO-enhanced MRI exceeds 95% for the detection of advanced HCCs with early enhancement [31]. In the present study, only 3 of the 88 HCCs with early enhancement (3.4%) were excluded from the study population. Second, the images were coarse in patients with decompensated liver cirrhosis because of the decrease in SPIO uptake by the liver parenchyma, similar to what happens in the case of Gd-EOB-DTPA-enhanced MRI. The indication of RFA for deteriorated liver cirrhosis is controversial, consequently Child–Pugh C cirrhotic patients were not included in the

present study. Third, artifacts sometimes appear in the ablated area (curvilinear hyperintense artifacts are indicated with arrowheads in Fig. 1). Central hyperintense artifacts, which usually look larger than the target tumors, can also appear. Even in such cases, the hypointense rim can still be considered to be the AM. Most of these types of artifacts can be distinguished from the ablated tumor by comparison with SPIO-enhanced MR images obtained before RFA. Although this can lead to an underestimation of the AM, it cannot lead to an overestimation. Forth, to get good-quality images, 17 s-breath hold is needed. Although it may be difficult for elderly patients, we could get evaluable images in all patients as it was easy to judge the white and black contrast even if the breath-hold was somewhat insufficient. Furthermore, our study also had a limitation that MRI and CT were reviewed by one of the board-certified radiologists belonging to our radiological department prospectively in daily practice. On this prospective judgement, we decided whether we should perform an additional treatment. Therefore, we could not perform the consensus reading or independent review by plural radiologists with the assessment of interobserver agreement.

In conclusion, RFA for HCCs was expected to be curative in patients with an AM thickness of 2 mm or more on MRI with pre-administered SPIO. In patients with AM(0) or AM less than 2 mm, additional ablation over a small area or careful follow-up is recommended, depending on patient preference and characteristics (e.g., liver function and age).

Author contribution KM and KF contributed equally. Study concepts, data analysis and manuscript drafting: KF and KM; acquisition of data and clinical studies: all authors; statistical analysis: NH; critical revision of the manuscript for important intellectual content: MA, MM, and IH; manuscript editing and final approval: all authors.

Funding This study was not supported by any grants.

Compliance with ethical standards

Conflict of interest All authors declare no potential conflict of interest.

Ethical statement This study was approved by the institutional ethics committee (H19-208) and was conducted in accordance with the ethical standards of the Declaration of Helsinki.

References

1. Cho YK, Rhim H, Noh S. Radiofrequency ablation versus surgical resection as primary treatment of hepatocellular carcinoma meeting the Milan criteria: a systematic review. J Gastroenterol Hepatol. 2011;26:1354–60.
2. Livraghi T, Meloni F, Di Stasi M, Rolle E, Solbiati L, Tinelli C, et al. Sustained complete response and complications rates after radiofrequency ablation of very early hepatocellular carcinoma in cirrhosis: is resection still the treatment of choice? Hepatology. 2008;47:82–9.
3. Feng K, Yan J, Li X, Xia F, Ma K, Wang S, et al. A randomized controlled trial of radiofrequency ablation and surgical resection in the treatment of small hepatocellular carcinoma. J Hepatol. 2012;57:794–802.
4. Chen MS, Li JQ, Zheng Y, Guo RP, Liang HH, Zhang YQ, et al. A prospective randomized trial comparing percutaneous local ablative therapy and partial hepatectomy for small hepatocellular carcinoma. Ann Surg. 2006;243:321–8.
5. Nakazawa T, Kokubu S, Shibuya A, Ono K, Watanabe M, Hidaka H, et al. Radiofrequency ablation of hepatocellular carcinoma: correlation between local tumor progression after ablation and ablative margin. Am J Roentgenol. 2007;188:480–8.
6. Mori K, Fukuda K, Asaoka H, Ueda T, Kunimatsu A, Okamoto Y, et al. Radiofrequency ablation of the liver: determination of ablative margin at MR imaging with impaired clearance of ferucarbotran-feasibility study. Radiology. 2009;251:557–65.
7. Hamm B, Staks T, Taupitz M, et al. Contrast-enhanced MR imaging of liver and spleen: first experience in humans with a new superparamagnetic iron oxide. J Magn Reson Imaging. 1994;4:659–68.
8. Mori K, Takahashi N, Hiratsuka M, Shiigai M, Minami M, Oda T, et al. Detection of hepatic metastases using ferucarbotran-enhanced MR imaging: feasibility and diagnostic accuracy of three-dimensional sensitivity-encoding water-excitation multishot echo-planar sequence (3D-SWEEP). J Magn Reson Imaging. 2006;24:1110–6.
9. Sasaki A, Kai S, Iwashita Y, Hirano S, Ohta M, Kitano S. Microsatellite distribution and indication for locoregional therapy in small hepatocellular carcinoma. Cancer. 2005;103:299–306.
10. Ochiai T, Takayama T, Inoue K, Yamamoto J, Shimada K, Kosuge T, et al. Hepatic resection with and without surgical margins for hepatocellular carcinoma in patients with impaired liver function. Hepatogastroenterology. 1999;46:1885–9.
11. Lee JW, Lee YJ, Park KM, Hwang DW, Lee JH, Song KB. Anatomical resection but not surgical margin width influence survival following resection for HCC, a propensity score analysis. World J Surg. 2016;40:1429–39.
12. Llovet JM, Burroughs A, Bruix J. Hepatocellular carcinoma. Lancet. 2003;362:1907–17.
13. Koda M, Tokunaga S, Miyoshi K, Kishina M, Fujise Y, Kato J, et al. Ablative margin states by magnetic resonance imaging with ferucarbotran in radiofrequency ablation for hepatocellular carcinoma can predict local tumor progression. J Gastroenterol. 2013;48:1283–92.
14. Shibata T, Isoda H, Hirokawa Y, Arizono S, Shimada K, Togashi K. Small hepatocellular carcinoma: is radiofrequency ablation combined with transcatheter arterial chemoembolization more effective than radiofrequency ablation alone for treatment? Radiology. 2009;252:905–13.
15. Tomonari A, Tsuji K, Yamazaki H, Aoki H, Kang JH, Kodama Y, et al. Feasibility of fused imaging for the evaluation of radiofrequency ablative margin for hepatocellular carcinoma. Hepatol Res. 2013;43:728–34.
16. Tang H, Tang Y, Hong J, Chen T, Mai C, Jiang P. A measure to assess the ablative margin using 3D-CT image fusion after radiofrequency ablation of hepatocellular carcinoma. HPB. 2015;17:318–25.
17. Wang XL, Li K, Su ZZ, Huang ZP, Wang P, Zheng RQ. Assessment of radiofrequency ablation margin by MRI-MRI image fusion in hepatocellular carcinoma. World J Gastroenterol. 2015;21:5345–51.
18. Nishigaki Y, Hayashi H, Tomita E, Suzuki Y, Watanabe N, Watanabe S, et al. Usefulness of contrast-enhanced ultrasonography using Sonazoid for the assessment of therapeutic response to

percutaneous radiofrequency ablation for hepatocellular carcinoma. Hepatol Res. 2015;45:432–40.
19. Koda M, Tokunaga S, Okamoto T, Hodozuka M, Miyoshi K, Kishina M, et al. Clinical usefulness of the ablative margin assessed by magnetic resonance imaging with Gd-EOB-DTPA for radiofrequency ablation of hepatocellular carcinoma. J Hepatol. 2015;63:1360–7.
20. Saxton RE, Huang A, Anzai Y, Castro DJ, Lufkin RB. Laser photothermal effects on stability and toxicity of magnetic resonance contrast agents. J Clin Laser Med Surg. 1995;13:363–6.
21. Merkle EM, Goldberg SN, Boll DT, Shankaranarayanan A, Boaz T, Jacobs GH, et al. Effects of superparamagnetic iron oxide on radiofrequency-induced temperature distribution: in vitro measurements in polyacrylamide phantoms and in vitro results in a rabbit liver model. Radiology. 1999;212:459–66.
22. Kakite S, Fujii S, Nakamatsu S, Kanasaki Y, Yamashita E, Matsusue E, et al. Usefulness of administration of SPIO prior to RF ablation for evaluation of the therapeutic effect: an experimental study using miniature pigs. Eur J Radiol. 2011;78:282–6.
23. Nagai M, Yamaguchi M, Mori K, Furuta T, Ashino H, Kurosawa H, et al. Magnetic resonance-based visualization of thermal ablative margins around hepatic tumors by means of systemic ferucarbotran administration before radiofrequency ablation: animal study to reveal the connection between excess iron deposition and T2*-weighted hypointensity in ablative margins. Invest Radiol. 2015;50:376–83.
24. Nayak AB, Luhar A, Hanudel M, Gales B, Hall TR, Finn JP, et al. High-resolution, whole-body vascular imaging with ferumoxytol as an alternative to gadolinium agents in a pediatric chronic kidney disease cohort. Pediatr Nephrol. 2015;30:515–21.
25. Garcia-Tsao G, Parikh CR, Viola A. Acute kidney injury in cirrhosis. Hepatology. 2008;48:2064–77.
26. D'Amico G, Garcia-Tsao G, Pagliaro L. Natural history and prognostic indicators of survival in cirrhosis: a systematic review of 118 studies. J Hepatol. 2006;44:217–31.
27. Mikami S, Tateishi R, Akahane M, Asaoka Y, Kondo Y, Goto T, et al. Computed tomography follow-up for the detection of hepatocellular carcinoma recurrence after initial radiofrequency ablation: a single-center experience. J Vasc Interv Radiol. 2012;23(10):1269–75.
28. Zhou P, Kudo M, Minami Y, Chung H, Inoue T, Fukunaga T, Maekawa K. What is the best time to evaluate treatment response after radiofrequency ablation of hepatocellular carcinoma using contrast-enhanced sonography? Oncology. 2007;72(Suppl 1):92–7.
29. Watanabe H, Kanematsu M, Goshima S, Yoshida M, Kawada H, Kondo H, Moriyama N. Is gadoxetate disodium-enhanced MRI useful for detecting local recurrence of hepatocellular carcinoma after radiofrequency ablation therapy? AJR Am J Roentgenol. 2012;198(3):589–95.
30. Midorikawa Y, Takayama T, Shimada K, Nakayama H, Higaki T, Moriguchi M, et al. Marginal survival benefit in the treatment of early hepatocellular carcinoma. J Hepatol. 2013;58:306–11.
31. Li YW, Chen ZG, Wang JC, Zhang ZM. Superparamagnetic iron oxide-enhanced magnetic resonance imaging for focal hepatic lesions: systematic review and meta-analysis. World J Gastroenterol. 2015;21:4334–44.